Journal of Alloys and Compounds 489 (2010) 530–534

Contents lists available at ScienceDirect

Journal of Alloys and Compounds

journal homepage: www.elsevier.com/locate/jallcom

Hydrothermal preparation and characterization of based-alloy Bi_2Te_3 nanostructure with different morphology

Masoud Salavati-Niasari[a,b,*], Mehdi Bazarganipour[b], Fatemeh Davar[a]

[a] Institute of Nano Science and Nano Technology, University of Kashan, Kashan, P.O. Box 87317–51167, Islamic Republic of Iran
[b] Department of Chemistry, University of Kashan, Kashan, P.O. Box. 87317–51167, Islamic Republic of Iran

ARTICLE INFO

Article history:
Received 19 August 2009
Received in revised form
11 September 2009
Accepted 14 September 2009
Available online 25 September 2009

Keywords:
Alloy
Bi_2Te_3
Hyrothermal

ABSTRACT

In this paper, based-alloy Bi_2Te_3 nanostructure with different morphologies was synthesized by a hydrothermal process based on the reaction between $Bi(NO_3)_3$, $TeCl_4$, and KBH_4 in water at various conditions. The products were characterized by X-ray diffraction (XRD), scanning electron microscopy (SEM), Fourier transform infrared spectrometry (FT-IR), X-ray photoelectron spectrum and inductively coupled plasma-atomic emission spectrometer and transmission electron microscopy (TEM). The result shows that the Bi_2Te_3 crystals have diameters ranging from 20 to 25 nm with high purity. Other factors, such as the reaction time, the different capping agent and the sort of reductant also have influence on the morphology of the final products to some extent. By variation of reductant, conversion rode-like to flower-like was obtained. Organic ligands play a manifold role in the formation of the chainlike nanostructures as both coordinate ligand and architecture template, and a possible formation mechanism is proposed.

1. Introduction

Thermoelectric (TE) materials are of interest for applications in cooling and electrical power generation devices due to many attractive features such as long life, no moving parts, no emissions of toxic gases, low maintenance, and high reliability [1,2]. The properties of the TE material is given to be a dimensionless figure of merit, $ZT = (\alpha^2\sigma/\kappa)T$, where α is the Seebeck coefficient, σ and κ the electrical and thermal conductivity, respectively, and T the absolute temperature. Bi_2Te_3-based alloys are the best-known TE materials for the applications in thermoelectric power generation and cooling near room temperature [3].

Many works have been done in recent years to improve the thermoelectric properties of them [4–6]. Based-nanoalloy Bi_2Te_3 with various morphologies has been reported recently using chemical routes, such as nanotubes by hydrothermal synthesis [7], sheets and rods by solvothermal synthesis [8,9] and nanocapsules by a low-temperature aqueous chemical method [10]. These chemical routes have the advantages of low cost, less device-dependence and large-scale synthesis. In the last decade, the preparations and properties of low dimensional TE materials have been intensively investigated, especially those of superlattice thin films and nanowire arrays. The narrow-gap-semiconductor Bi_2Te_3 (band gap: $E_g = 0.15$ eV) and its alloys are the best room-temperature bulk thermoelectric materials found to date [11].

Recently, solvothermal or hydrothermal synthesis has been used to prepare Bi_2Te_3 based-nanoalloy and much different morphology have been obtained, including nanorods, polygonal nanosheets, nanoplates, polyhedral nanoparticles and sheet-rods [12–16]. Some possible mechanisms of formation of Bi_2Te_3 alloy, such as "mono-atom model" and "continuous nucleation model", have been proposed [13–17]. In this work, we reported on based-alloy Bi_2Te_3 nanostructure prepared by the simpler hydrothermal method, and compared the difference in the nanostructure of Bi_2Te_3 synthesized with different sort of reductant.

2. Experimental

2.1. Materials and physical measurements

All of reagents and solvents were purchased from Merck (pro-analysis) and were dried using molecular sieves (Linde 4 Å). The metallic impurities were identified by inductively coupled plasma-optical emission spectrometer (ICP-OES) Model PerkinElmer PLASMA-1000. XRD patterns were recorded by a Rigaku D-max C III, X-ray diffractometer using Ni-filtered Cu Kα radiation. Scanning electron microscopy (SEM) images were obtained on Philips XL-30ESEM equipped with an energy dispersive X-ray spectroscopy. Transmission electron microscopy (TEM) images were obtained on a Philips EM208 transmission electron microscope with an accelerating voltage of 100 kV. Fourier transform infrared (FT-IR) spectra were recorded on Shimadzu Varian 4300 spectrophotometer in KBr pellets. X-ray energy dispersive spectroscopy (EDS) analysis with 20 kV accelerated voltage. X-ray photoelectron

* Corresponding author at: Institute of Nano Science and Nano Technology, University of Kashan, Kashan, P.O. Box. 87317–51167, Islamic Republic of Iran.
Tel.: +98 361 5555 333; fax: +98 361 555 29 30.
E-mail address: salavati@kashanu.ac.ir (M. Salavati-Niasari).

0925-8388/$ – see front matter © 2009 Elsevier B.V. All rights reserved.
doi:10.1016/j.jallcom.2009.09.101

spectrum (XPS) was collected on an ESCALab MKII X-ray photoelectron spectrometer, using nonmonochromatized Mg Kα X-ray as the excitation source and C 1s (284.6 eV) as the reference line.

2.2. Based-alloy Bi_2Te_3 nanostructure prepared by hydrothermal method

$Bi(NO_3)_3$ and $TeCl_4$ were used as the simple precursor in the hydrothermal synthesis. The precursor with stoichiometric ratio of Bi:Te (2:3) was put into a Teflon-lined autoclave. The autoclave was then filled with water up to 80% of its volume. After adding sufficient KBH_4 as the reductant and propane-1,3-diamine (pn) as complex agent, the autoclave was sealed immediately and heated to 150 °C for the synthesis reaction. After reaction for 24 h, the autoclave was cooled down to room temperature naturally. The obtained precipitates were separated by centrifugation, washed with deionized water followed by ethanol for three times, and dried at 100 °C under vacuum for 24 h. The structure and morphology of the Bi_2Te_3 powders were characterized by XRD and TEM.

3. Result and discussion

The composition of the as-prepared product was determined by XRD (Fig. 1a). All peaks in the patterns correspond to the reflections of rhombohedral phase Bi_2Te_3 [space group: R 3m (1 6 6)], with lattice constants $a = 0.4386$ nm and $c = 3.056$ nm, compatible with the literature values of $a = 0.4385$ nm and $c = 3.048$ nm (JCPDS 15-0863). No remarkable diffractions of other phases such as tellurium, bismuth or their other compounds can be found in Fig. 1a, indicating that a pure Bi_2Te_3 phase has been formed after the synthesis for all samples. The broadening of the diffraction peaks indicates that the samples are nanosized. The average particle size of the sample is about 23 nm, estimated through the Scherrer formula. Meanwhile, influence of capping agent and temperature was investigated on the as-prepared alloy Bi_2Te_3 (Fig. 1b–e). With exchange of capping agent from PEG 600 to PEG 20000, particle size of 19–18 nm would be decreased, respectively (Fig. 1b and c). In other word, with increasing of temperature from 120 °C to 180 °C, particle size of 17.5–31 nm would be increased, respectively (Fig. 1d and e). Obviously, the crystallinity of the as-prepared Bi_2Te_3 gradually improved with increasing reaction temperature. In general the resultant particles became bigger with increasing temperature.

The morphology and size of the as-synthesized products were characterized by SEM and TEM. Fig. 2 depicts SEM images of sample alloy Bi_2Te_3. From the micrograph, it was observed that the alloys were slightly agglomerated. Fig. 2 reveals temperature effect on morphology of nanoalloys. With increasing reaction temperature from 120 °C to 150 °C, alloys show dense agglomerate and particle size was increased (Fig. 2a–d). Fig. 2b shows that the Bi_2Te_3 powder obtained at 150 °C are quasi-spherical with particle size about 25 nm. In other side, for reach ideal morphology, we prepared nano-size Bi_2Te_3 alloy with various capping agents such as: PEG 600 and PEG 20000 in the presence of KBH_4 as reductant (Fig. 3a and b). Fig. 3a and b shows that, utilization of PEG 20000, decline agglomeration of alloys and growing of particle. In continues, effect of reductant sort was investigated on morphology nanoalloys in the presence of PEG 20000 as capping agent. In this study, reductant plays the key role on morphology of Bi_2Te_3 alloys. In the presence of N_2H_4 as reductant, the rode-like shape is preferential morphology along with agglomeration of particles (Fig. 3c). Meanwhile, in the presence of Zn as reductant flower-like is preferential morphology (Fig. 3d). In other side, effect of time on morphology Bi_2Te_3 nanoalloys was investigated. For instance, by using Zn as reductant, with increasing period of time from 12 to 48 h, flower-like morphology damaged to large particle size (Fig. 4a and b). In other word, in the presence of N_2H_4 as reductant, with increasing period of time from 12 to 48 h, rode-like alloy breaks down and agglomerated (Fig. 4c and d).

The formation of the flower-like based-alloys Bi_2Te_3 during the hydrothermal synthesis should be related to the layered anisotropic

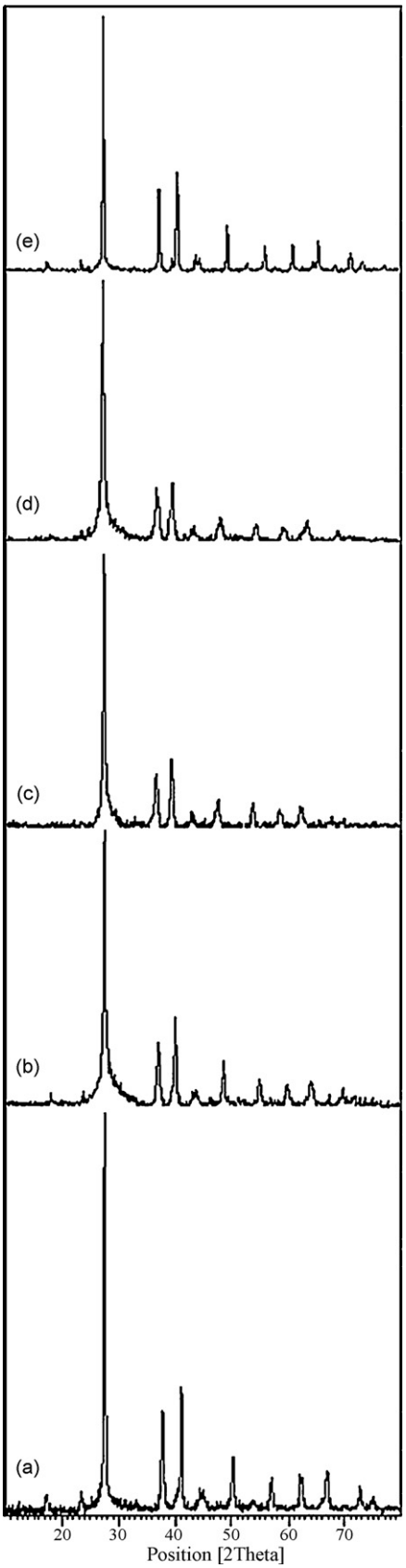

Fig. 1. XRD patterns of prepared Bi_2Te_3 in (a) 150 °C in the presence of pn as capping agent, (b) 150 °C in the presence of PEG 600 as capping agent, (c) 150 °C in the presence of PEG 20000 as capping agent, (d) 120 °C in the presence of PEG 20000 as capping agent, and (e) 180 °C and KBH_4 as reductant.

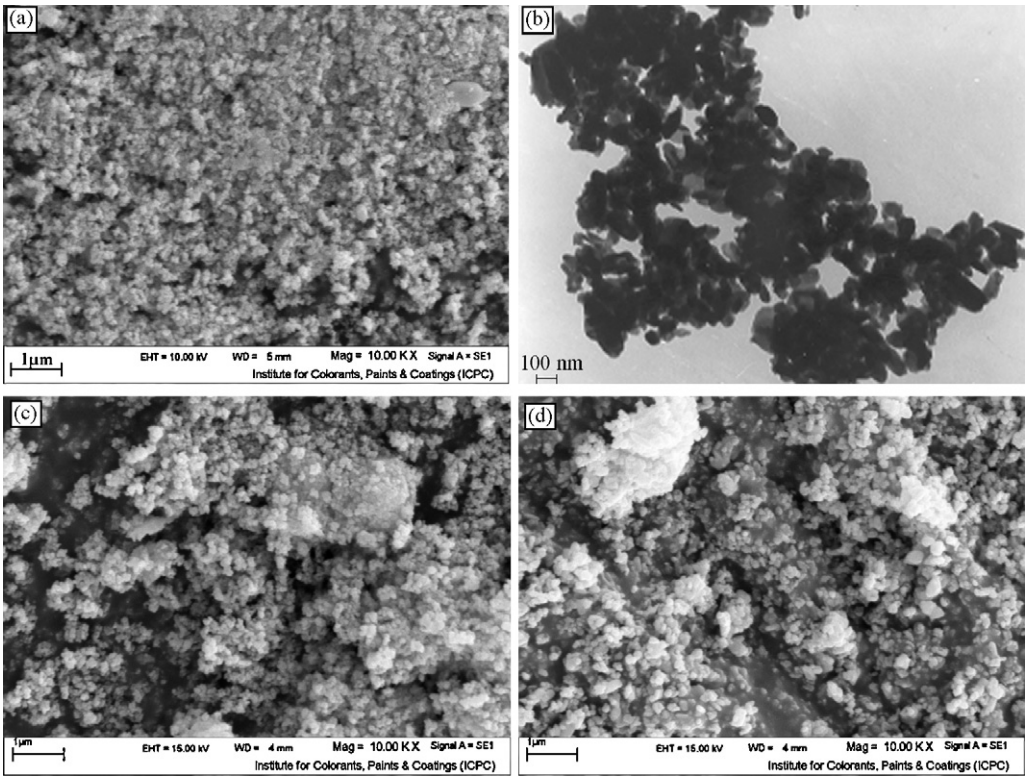

Fig. 2. (a, b) SEM and TEM image of images of Bi_2Te_3 in presence of KBH_4 as reductant and pn as capping agent at 120 °C and (c, d) SEM image at 150 °C and 180 °C respectively.

lattice structure. During the synthesis process, a free Te atom or Te^{2-} ion tends to bond with the atoms on the growing crystal surface via covalent bonding. A single Te atom or Te^{2-} ion from the solution attaching itself to a Te layer crystal surface will probably jump back into the solution, since a van der Waals bonding is not strong enough to hold the atom on the atomic surface. Therefore, a Bi_2Te_3 crystal will grow faster in the *a*- and *b*-axis directions than in the *c* direction [18].

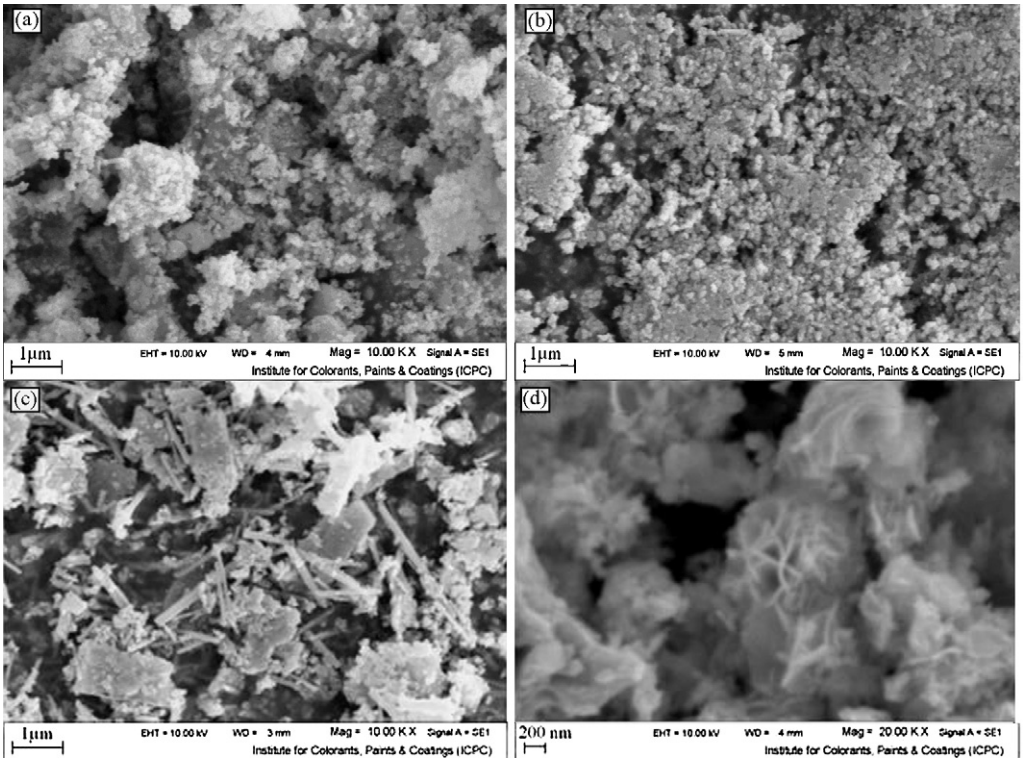

Fig. 3. SEM images of Bi_2Te_3 in (a) PEG 600 and (b) PEG 20000 in 150 °C and KBH_4 as reductant, in the presence of (c) N_2H_4 and (d) Zn as reductant in 150 °C and PEG 20000 as capping agent.

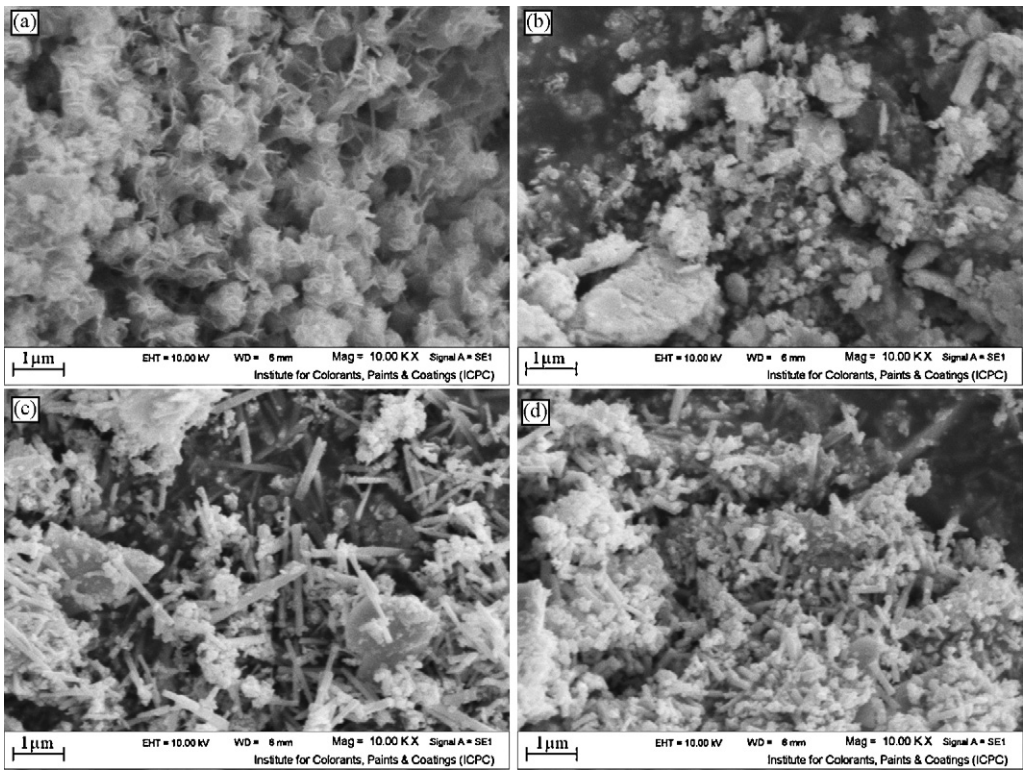

Fig. 4. SEM images of Bi_2Te_3 (a) Zn, 12 h; (b) Zn, 48 h; (c) N_2H_4, 12 h; and (d) N_2H_4, 48 h in the presence of PEG 20000 as capping agent and 150 °C.

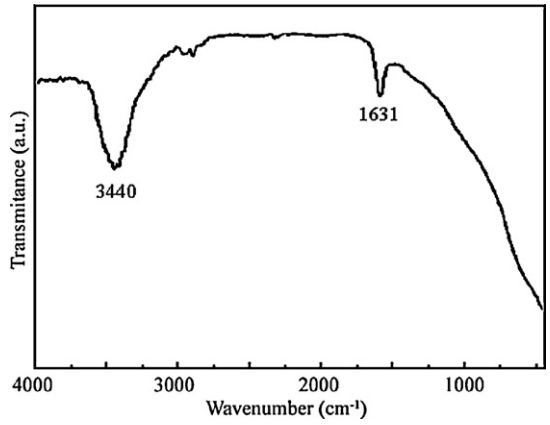

Fig. 5. FT-IR spectra of prepared based-alloy Bi_2Te_3 nanostructure in the presence of pn as capping agent.

The advantage of the wet preparation method is that the reduced metal cations are homogeneously dissolved in a solution. Whereas the reduction with KBH_4 and $N_2H_4{\cdot}H_2O$ proceeded in a homogeneous way, the metal cation solution and the reductant solution were liquid and the reduction of the liquid metal cation solution with the solid Zn powder was a heterogeneous process being limited by the interface area of the Zn surface and the solution in contact with this surface. The consequences may be dramatic. The strong reductant KBH_4 and $N_2H_4{\cdot}H_2O$ in combination with stirring rapidly create a large number of nuclei and further growth of the nuclei is limited. As a result, many small particles are obtained. The reduction at the presence of Zn proceeds only two-dimensionally, i.e., at the interface of Zn powder with the metal cation solution. The rate of reduction is further limited by the mass transport of the metal cation solution to the Zn surface. Therefore, depletion of metal cations near the interface might occur. As a consequence of the rate and surface area limitation, crystal growth is favored over nucleus formation as the result of larger particles [19].

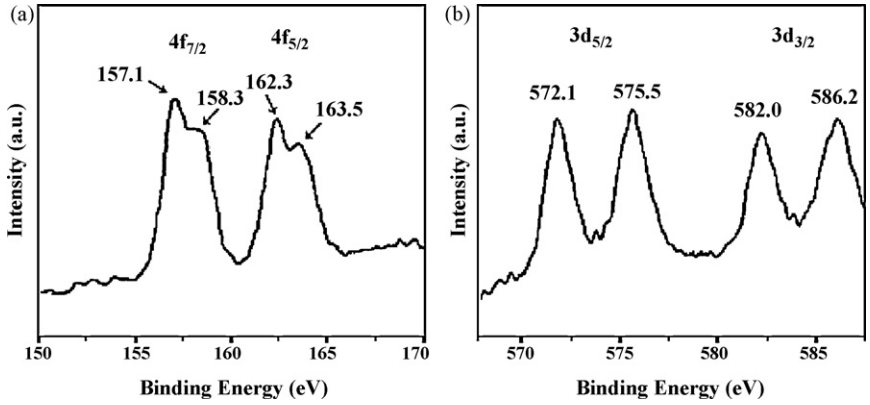

Fig. 6. (a) XPS of Bi the 4f core level in Bi_2Te_3 nanocrystallines and (b) XPS of the Te 3d core level in Bi_2Te_3 nanocrystallines.

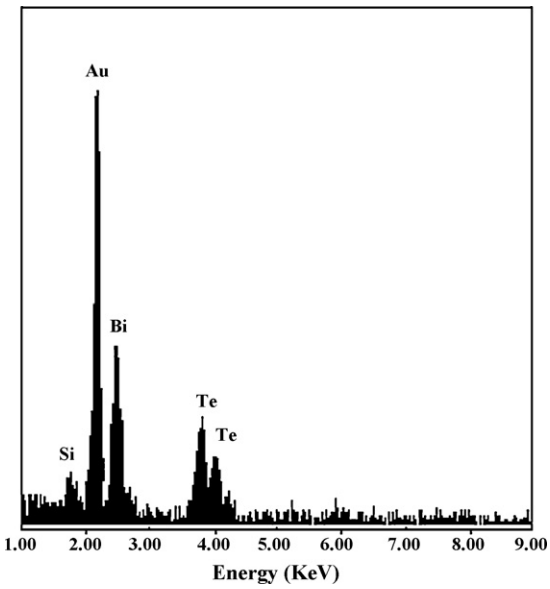

Fig. 7. EDS pattern of Bi_2Te_3 alloys.

While it is believed that the surfactant could prevent the aggregation of Bi_2Te_3 nuclear at first. In addition, propane-1,3-diamine molecules might be able to modulate the growth kinetics of the Bi_2Te_3 seeds, as controlled probably by their different adsorption energies on various basal planes of this rhombohedral structure, and modify the surface chemical properties. When propane-1,3-diamine was added into the solution, it would adsorb to the growing nuclear easily. Fig. 5 shows a typical FT-IR spectrum of as-prepared Bi_2Te_3 nanocrystals in this system with propane-1,3-diamine. The sample was washed with absolute ethanol and distilled water several times, and then dried in a vacuum before used. Though the peaks could be assigned to propane-1,3-diamine molecules adsorbed on Bi_2Te_3 nanocrystals, the NH_2 peak ($1631\,cm^{-1}$) became weaker, and it shifted to some extend. This phenomenon might result from the interaction of N–Te on the top and bottom of the nuclear surface. Due to layer-like structure and weak van derWaals force along *c*-axis, the propane-1,3-diamine molecule might adsorb to these crystal planes, and significantly decrease the growth rates along *c*-axis. In the other way, the growth perpendicular to *c*-axis would be induced and also enhanced. Therefore, after the reaction was completed, rhombohedral Bi_2Te_3 nanocrystals were finally obtained.

Fig. 6a shows the photoelectron spectrum of Bi 4f. The two higher peaks at energy of 157.1 and 162.3 eV, corresponding to the binding energy of Bi $4f_{7/2}$ and Bi $4f_{5/2}$ of Bi_2Te_3, are in good agreement with data observed from Bi_2Te_3 single crystal [16]. The two lower energy peaks at 158.3 and 163.5 eV, are in good agreement with a Bi 4f spectra of an oxidized layer of Bi_2Te_3 [20]. Fig. 6b shows the photoelectron spectrum of the Te 3d core level. The two peaks at energies of 572.1 and 582.0 eV are in good agreement with the binding energies seen in the Te 3d spectra observed from Bi_2Te_3 single crystals. The other two peaks at energies of 575.5 and 586.2 eV are in good agreement with the Te 3d spectra from an oxidized layer of Bi_2Te_3. All four peaks had been observed by Bando et al. [20]. The relative peak intensities in the XPS spectra of the nanocrystalls are analogous to the samples which were cleaved and then oxidized in desiccator for 56 h at room temperature [20]. The atoms at surface are more active compared to inter atoms, so samples obtained are more easily oxidized in air due to their surface-to volume [21]. The ICP-atomic emission spectroscopy shows that the atom ratio of products is Bi:Te = 1:1.49, which is close to the value for the stoichiometric compound. We can therefore conclude from results that the product obtained is Bi_2Te_3, but the outside layers of the particles are oxidized.

X-ray energy dispersive spectroscopy (EDS) analysis measurement was used to characterize the chemical composition of the products (Fig. 7). The results show that there exist only elements Bi and Te and the atomic ratio of Bi to Te in different areas is always 38.63:61.09, which indicates a purity Bi_2Te_3 phase in the rods. In addition, neither N nor C signals were detected in the SEDX spectrum, which means there exist no solvent or propane-1,3-diamine ligand in the rod crystals.

In comparison to other similar works, our method is simple and has low cost and scale-up route. Also, we have used nontoxic precursor and solvent. In this route, we apply various capping agent and sort of reductant which are rare in preparation of based-alloy Bi_2Te_3 nanostructure and different morphology such as: rode-like and flower-like was obtained. The sizes of based-alloy Bi_2Te_3 nanostructure seem convenient than similar works.

4. Conclusion

In summary, this work has demonstrated a new approach for the controllable growth of Bi_2Te_3 rod-like and flower-like via exchange reductant. This route to based-alloy Bi_2Te_3 nanostructure is simple, convenient and effective, and holds potential for large-scale synthesis needed for commercial applications. Most important of all, the new approach can yield rode-like and flower-like morphology of Bi_2Te_3 directly without the mechanical crushing and the sieving need for a solidified melt which may exhibit enhanced thermoelectric properties.

Acknowledgment

Authors are grateful to Council of Institute of Nano Science and Nano Technology, University of Kashan and for providing financial support to undertake this work.

References

[1] Z. Chai, Z. Peng, C. Wang, H. Zhang, Mater. Chem. Phys. 113 (2009) 664–669.
[2] B.C. Sales, Science 295 (2002) 1248–1249.
[3] T.M. Tritt, Science 283 (1999) 804–805.
[4] E. Koukharenko, N. Fréty, V.G. Shepelevich, J.C. Tedenac, J. Alloys Compd. 299 (2000) 254–257.
[5] J.Y. Yang, T. Aizawa, A. Yamamoto, T. Ohta, J. Alloys Compd. 312 (2000) 326–330.
[6] D.-Y. Chung, T. Hogan, P. Brazis, M. Rocci-Lane, C. Kannewurf, M. Bastea, C. Uher, M.G. Kanatzidis, Science 287 (2000) 1024–1027.
[7] X.B. Zhao, X.H. Ji, Y.H. Zhang, T.J. Zhu, J.P. Tu, X.B. Zhang, Appl. Phys. Lett. 86 (2005) 1–3.
[8] Y. Deng, C.W. Nan, G.D. Wei, L. Guo, Y.H. Lin, Chem. Phys. Lett. 374 (2003) 410–415.
[9] Y. Deng, G.D. Wei, C.W. Nan, Chem. Phys. Lett. 368 (2003) 639–643.
[10] X.B. Zhao, T. Sun, T.J. Zhu, J.P. Tu, J. Mater. Chem. 15 (2005) 1621–1625.
[11] H.J. Goldsmil, Electronic Refrigeration, Pion, London, 1986.
[12] S.H. Yu, J. Yang, Y.S. Wu, Z.H. Han, J. Lu, Y. Xie, Y.T. Qian, J. Mater. Chem. 8 (1998) 1949–1951.
[13] Y. Deng, X.S. Zhou, G.D. Wei, J. Liu, C.W. Nan, S.J. Zhao, J. Phys. Chem. Solids 63 (2002) 2119–2122.
[14] Y. Xu, Z. Ren, W. Ren, G. Cao, K. Deng, Y. Zhong, Mater. Lett. 62 (2008) 4273–4276.
[15] X.B. Zhao, Y.H. Zhang, X.H. Ji, Inorg. Chem. Commun. 7 (2004) 386–388.
[16] X.B. Zhao, X.H. Ji, Y.H. Zhang, B.H. Lu, J. Alloys Compd. 368 (2004) 349–352.
[17] X.B. Zhao, X.H. Ji, Y.H. Zhang, G.S. Cao, J.P. Tu, Appl. Phys. A: Mater. Sci. Process 80 (2005) 1567–1571.
[18] Y.H. Zhang, T.J. Zhu, J.P. Tu, X.B. Zhao, Mater. Chem. Phys. 103 (2007) 484–488.
[19] A. Trifonova, M. Wachtler, M.R. Wagner, H. Schroettner, Ch. Mitterbauer, F. Hofer, K.-C. Möller, M. Winter, J.O. Besenhard, Solid State Ionics 168 (2004) 51–59.
[20] H. Bando, K. Koizumi, Y. Oikawa, K. Daikohara, V.A. Kulbachinskii, H. Ozaki, J. Phys.: Condens. Mater. 12 (2000) 5607–5616.
[21] T. Sugimoto, Fine Particles: Synthesis Characterization and Mechanisms of Growth, Marcel Dekker, New York, 2000.